ACTA
PROTOZOOLOGICA

Acta Protozool. (2013) 52: 73–89
http://www.eko.uj.edu.pl/ap
doi:10.4467/16890027AP.13.008.1087

Taxonomic Descriptions of Two Marine Ciliates, *Euplotes dammamensis* n. sp. and *Euplotes balteatus* (Dujardin, 1841) Kahl, 1932 (Ciliophora, Spirotrichea, Euplotida), Collected from the Arabian Gulf, Saudi Arabia

Xiangrui CHEN[1], Yan ZHAO[2], Saleh A. AL-FARRAJ[3], Saleh A. AL-QURAISHY[3], Hamed A. EL-SEREHY[3], Chen SHAO[4] and Khaled A. S. AL-RASHEID[3]

[1]School of Marine Science, Ningbo University, Ningbo, China; [2]Laboratory of Protozoology, Institute of Evolution & Marine Biodiversity, Ocean University of China, Qingdao, China; [3]Zoology Department, King Saud University, Riyadh, Saudi Arabia; [4]The Key Laboratory of Biomedical Information Engineering, Ministry of Education, School of Life Science and Technology, Xi'an Jiaotong University, Xi'an, China

Abstract. The morphology, morphogenesis and infraciliature of two marine euplotid ciliates, *Euplotes dammamensis* n. sp. and *Euplotes balteatus* (Dujardin, 1841) Kahl, 1932, isolated from a sandy beach of the Arabian Gulf, Saudi Arabia, were investigated using observations *in vivo* and protargol-impregnation methods. *Euplotes dammamensis* n. sp. is characterized by a combination of features including its huge body size (100–170 × 80–120 μm), 10 conspicuous dorsal ridges, 10 normal-sized frontoventral and two marginal cirri, and 11 dorsal kineties. *Euplotes balteatus* is mainly characterized by 10 frontoventral, two caudal, and two left marginal cirri, 7–10 dorsal kineties and 5–7 prominent dorsal ridges as well as double-eurystomus silverline system. The small subunit rRNA (SSU-rRNA) gene sequences were determined for both species and phylogenetic analyses based on these data indicated that *E. dammamensis* is most closely related to *E. parabalteatus* Jiang *et al*., 2010, and *E. balteatus* clusters with *E. plicatum* Valbonesi *et al*., 1997, *E. orientalis* Jiang *et al*., 2010, and *E. bisulcatus* Kahl, 1932.

Key words: Marine ciliate, morphogenesis, morphology, new species, SSU-rRNA, taxonomy.

Address for correspondence: Khaled A. S. Al-Rasheid, Zoology Department, King Saud University, Riyadh 11451, Saudi Arabia. E-mail: krasheid@ksu.edu.sa
Address for co-correspondence: Chen Shao, The Key Laboratory of Biomedical Information Engineering, Ministry of Education, School of Life Science and Technology, Xi'an Jiaotong University, Xi'an 710049, China. E-mail: shaochen@mail.xjtu.edu.cn

INTRODUCTION

Euplotes Ehrenberg, 1830 is a highly diversified and cosmopolitan genus, with a large number of species that have been observed and investigated in all kinds of biotopes. Traditionally, they are characterized by their body size and body shape, their dorsal and ventral ridges, and the cirral pattern on the ventral side. With the improvement in research methods during the last half century, some new specific features have been used to distinguish this kind of organism, such as: the numbers and arrangement of the cirri on the ventral surface; the shape of the adoral zone of membranelles and the number of membranelles; the shape of the macronucleus; the number of dorsal kineties; the silverline system pattern (Tuffrau 1960, Borror 1972, Carter 1972, Curds 1975). Based on these characteristics, more than 30 new morphospecies of *Euplotes* have been reported in the last three decades (Berger and Foissner 1989; Agatha *et al*. 1990; Valbonesi and Luporini 1990, 1995; Petz *et al*. 1995; Coppellotti and Cisotto 1996; Song and Bradbury 1997; Song and Packroff 1997; Song and Wilbert 1997, 2002; Valbonesi *et al*. 1997; Lobban *et al*. 2005; Schwarz and Stoeck 2007; Schwarz *et al*. 2007; Wilbert and Song 2008; Jiang *et al*. 2010a, b; Shao *et al*. 2010; Pan *et al*. 2012).

In the present study two *Euplotes* species were isolated from a sandy beach of the Arabian Gulf, Saudi Arabia, including one new species. These are described following examination of live and protargol-impregnated specimens, small subunit rRNA (SSU-rRNA) gene sequence homology and the phylogenetic relationship with their congeners.

MATERIALS AND METHODS

Morphological and morphogenetic studies

Euplotes dammamensis n. sp. and *E. balteatus* were collected on 16 December 2011 from the intertidal regions of a sandy beach on the Arabian Gulf (Dammam, Saudi Arabia, 26°33′07″N, 50°01′30″E) where the water temperature was 17°C and the salinity 65‰ (In general, the salinity of the Arabian Gulf is about 38–41‰. The sampling location, however, is an intertidal sandy pool, and the salinity is, therefore, higher than in open waters). The upper 5 cm layer of sand was collected together with seawater from the site. Specimens were maintained in Petri dishes at room temperature (about 20°C) with added rice grains to enrich bacteria as food for the ciliates (Chen *et al*. 2012). Attempts to culture the two species failed; therefore all studies were carried out on freshly isolated specimens.

Isolated individuals were examined *in vivo* using bright field and Nomarski differential interference contrast microscopy. The protargol-impregnation method of Wilbert (1975) was used in order to reveal the infraciliature. Counts and measurements on stained specimens were performed at a magnification of 1,250 ×. Drawings were made with the help of a camera lucida. Terminology is mainly according to Curds (1975).

SSU-rRNA gene sequence analysis

Genomic DNA extraction, PCR amplification, and SSU-rRNA gene amplification and sequencing of *Euplotes dammamensis* n. sp. and *E. balteatus* were performed according to Huang *et al*. (2012). The primers used for SSU-rRNA gene amplification were Eukaryotic universal A (5'-AAC CTG GTT GAT CCT GCC AGT-3') and Eukaryotic universal B (5'-TGA TCC TTC TGC AGG TTC ACC TAC-3') covering the full length of the gene by polymerase chain reaction (PCR) (Medlin *et al*. 1988). The new sequences have been deposited in the GenBank database (*E. dammamensis*: JX185743, *E. balteatus*: JX185744). The other nucleotide sequences used in this study and their GenBank/EMBL accession numbers are given after the names of the species in figure 91.

Alignment was performed using MUSCLE alignment implemented in Geneious v5.4 (Drummond *et al.* 2010). The resulting alignment was manually inspected using the software Mega v5.0 (Tamura *et al.* 2011). The alignment results of congeners morphologically similar to those in the present study have been set out in Table 3. The datasets used for SSU-rRNA phylogenetic analyses included 1,582 positions. *Loxodes striatus* (U24248) was selected as the out-group species. A Bayesian inference (BI) analysis was performed with MrBayes 3.1.2 (Ronquist and Huelsenbeck 2003) using the GTR+I+G model selected by MrModeltest 2 (Nylander 2004) under the AIC criterion. Markov chain Monte Carlo (MCMC) simulations were run with two sets of four chains using the default settings: chain length 1,000,000 generations, with trees sampled every 100 generations. The first 2,500 trees were discarded as burn-in. The remaining trees were used to generate a consensus tree and to calculate the posterior probabilities (PP) of all branches using a majority-rule consensus approach. A Maximum Likelihood (ML) analysis was performed with PhyML v3.0 (Guindon and Gascuel 2003) using the GTR+G+I model selected under the AIC criterion by Modeltest v.3.7 (Posada and Crandall 1998). BIONJ was used to obtain starting trees and BEST was selected for branch swapping. The reliability of internal branches was assessed using a non-parametric bootstrap method with 1,000 replicates. Finally, phylogenetic trees (BI and ML) were visualized and edited in Geneious v5.4 (Drummond *et al*. 2010).

RESULTS AND DISCUSSION

Euplotes dammamensis n. sp. (Figs 1–36; Tables 1, 2)

Diagnosis. Marine *Euplotes* with 10 conspicuous dorsal ridges, 100–170 × 80–120 μm *in vivo*. Adoral zone comprising about three-quarters of the total cell length, with about 48 membranelles; consistently 10 frontoventral, five transverse and two marginal cirri,

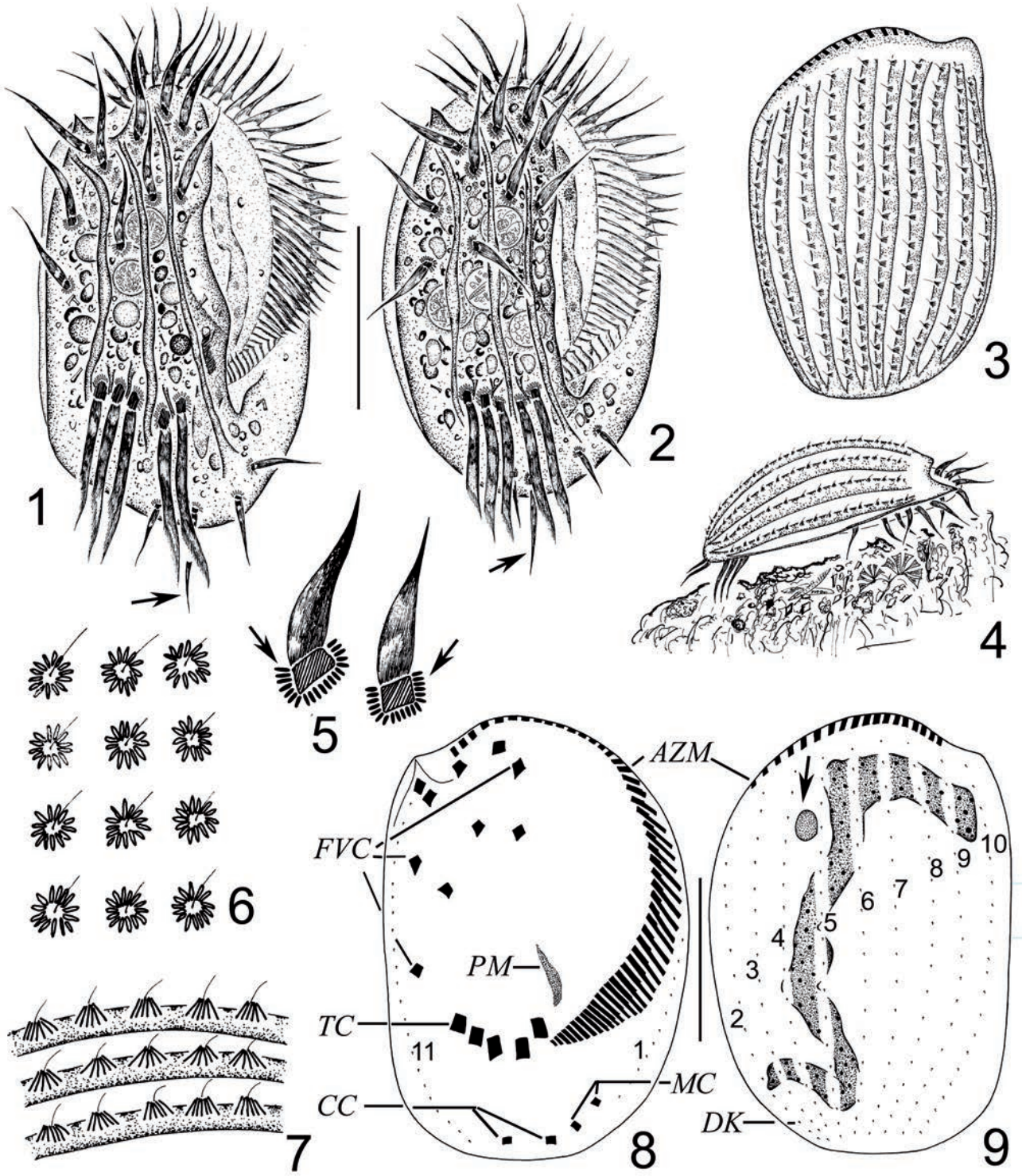

Figs 1–9. *Euplotes dammamensis* n. sp. *in vivo* (1–7) and after protargol impregnation (8, 9). **1**, **2** – ventral views of different individuals, arrows indicate the longest caudal cirrus; **3** – dorsal view, showing the conspicuous ridges; **4** – lateral view; **5** – frontoventral cirri, arrows indicate the cortical granules around the cirri; **6** – apical view of the cortical granules distributed on the dorsal side; **7** – lateral view of the cortical granules; **8**, **9** – ventral and dorsal views of the same specimen, showing the general infraciliature and the micronucleus (arrow). AZM – adoral zone of membranelles, CC – caudal cirri, DK – dorsal kineties, FVC – frontoventral cirri, MC – marginal cirri, PM – paroral membrane, TC – transverse cirri, 1–11 – dorsal kineties. Scale bars: 50 μm.

Table 1. Morphometric data for *Euplotes dammamensis* n. sp. (upper rows) and *E. balteatus* (lower rows). Min – Minimum, Max – maximum, Mean – arithmetic mean, SD – standard deviation, SE – standard error of arithmetic mean, CV – coefficient of variation (%), n – number of individuals examined.

Characteristic	Min	Max	Mean	SD	SE	CV	n
Cell length, μm	107	165	127.4	12.22	2.3	9.6	28
	76	99	85.6	5.75	1.1	6.7	25
Cell width, μm	80	111	94.8	6.52	1.2	6.9	28
	56	73	62.8	3.85	0.8	6.1	25
Length of adoral zone, μm	82	112	95.0	6.21	1.2	6.5	28
	55	70	62.1	3.88	0.8	6.2	25
Length of paroral membrane, μm	18	24	20.4	1.43	0.3	7.0	28
	8	13	10.6	1.08	0.2	10.2	25
Number of adoral membranelles	44	51	48.3	1.80	0.3	3.7	28
	31	39	34.8	1.76	0.4	5.1	25
Number of frontoventral cirri	10	10	10.0	0	0	0	28
	10	10	10.0	0	0	0	25
Number of transverse cirri	5	5	5.0	0	0	0	28
	5	5	5.0	0	0	0	25
Number of marginal cirri	2	2	2.0	0	0	0	28
	2	2	2.0	0	0	0	25
Number of caudal cirri	2	3	2.2	0.39	0.1	17.7	28
	2	2	2.0	0	0	0	25
Number of dorsal kineties	11	11	11.0	0	0	0	28
	7	7	7.0	0	0	0	25
Number of dikinetids in mid-dorsal kinety	14	18	16.0	1.12	0.2	7.0	28
	10	13	11.2	0.88	0.2	7.9	25
Number of dikinetids in leftmost dorsal kinety	10	13	11.2	1.07	0.2	9.6	28
	4	7	5.1	0.99	0.2	19.4	25
Number of dikinetids in second rightmost dorsal kinety	17	24	20.4	1.57	0.3	7.7	28
	12	15	13.1	0.95	0.2	7.3	25
Number of dikinetids in rightmost dorsal kinety	17	22	19.7	1.38	0.3	7.0	28
	10	13	12.0	0.89	0.2	7.4	25

Data are based on protargol-impregnated specimens.

and, generally, two or three caudal cirri, with second cirrus prolonged significantly; 11 dorsal kineties with about 16 dikinetids in mid-dorsal row. Macronucleus variable in shape, anterior part typically C-shaped with posterior part distorted.

Type location. Isolated from the Arabian Gulf (26°33′07″N, 50°01′30″E) on 16 December 2011. Salinity about 65‰ and water temperature about 17°C.

Type specimens. The slide (registration number: CXR-20111216-20-01) containing the holotype specimen (Figs 8, 9, 27, 28) and one paratype slide (registration number: CXR-20111216-20-02) with protargol-impregnated specimens have been deposited in the Laboratory of Protozoology, Ocean University of China, Qingdao.

Etymology. The species-group name *dammamensis* refers to the area (Dammam, Saudi Arabia) where the sample was collected.

Morphological description. Cells *in vivo* usually 130–150 μm long. Outline in frontal plane broadly elliptical to doliform (Figs 1, 19); left and right margins usually convex in well-fed individuals (Figs 2, 20); anterior end with a distinct projection on right side (Figs 1, 2, 19). Cell dorsoventrally flattened about 2:1 with ventral side straight or slightly convex and dorsal side strongly arched (Figs 4, 22). Ventral side with three conspicuous ridges, two right ridges extending posteriorly to transverse cirri, and leftmost ridge extending to marginal cirri (Figs 1, 2, 19, arrowheads); ridges among transverse cirri short but prominent. Dorsal side usually

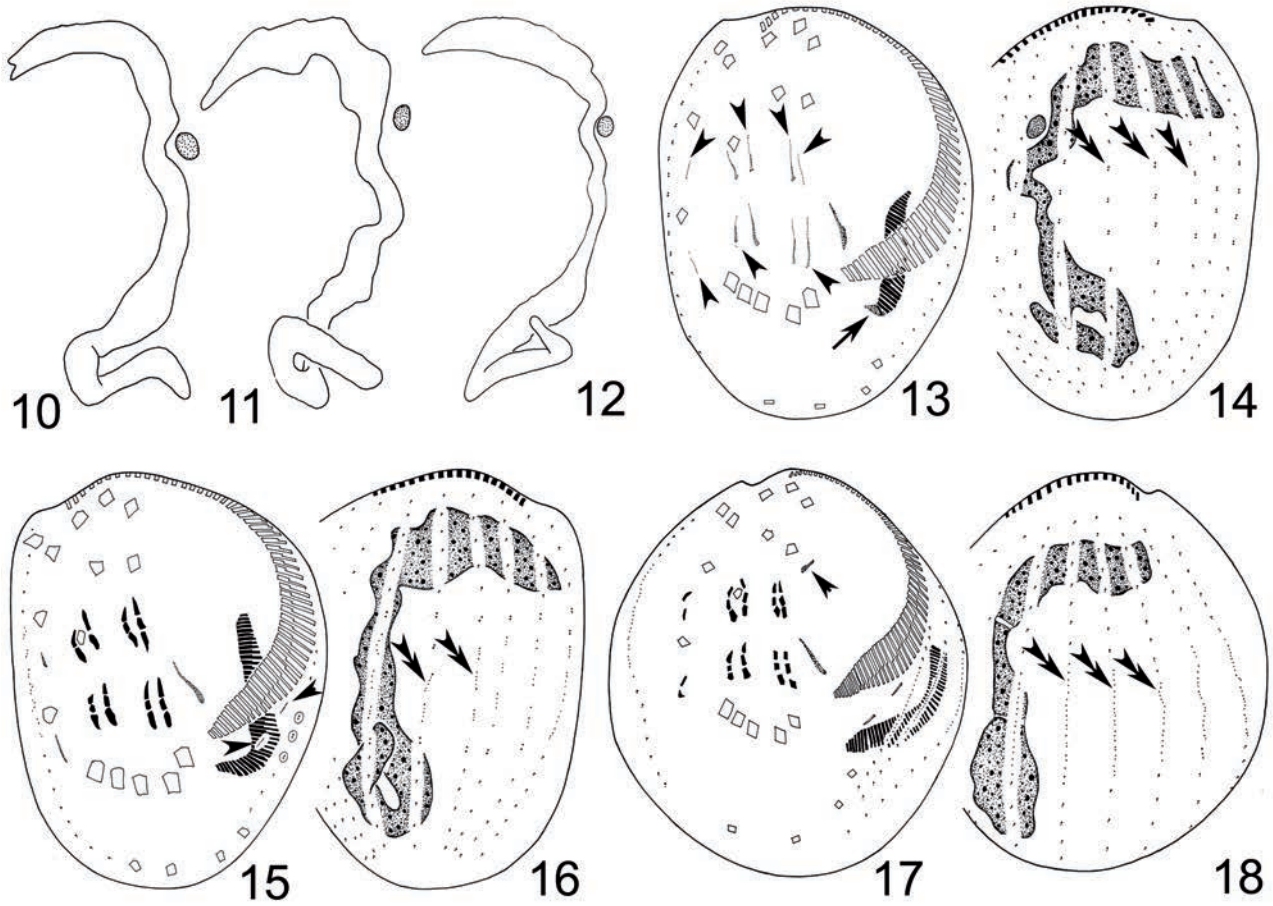

Figs 10–18. Morphogenesis and macronucleus of *Euplotes dammamensis* n. sp. after protargol impregnation. **10–12** – different shapes of macronucleus; **13**, **14** – ventral and dorsal views of the same specimen at an early stage of morphogenesis, showing the appearance of frontoventral-transverse cirral anlagen (arrowheads), the developing oral primordium (arrow) and the proliferation of basal bodies in the dorsal kineties (double-arrowheads); **15**, **16** – ventral and dorsal views of the same specimen showing the marginal cirral anlagen (arrowheads) and the newly formed dorsal kinety anlagen (double-arrowheads); **17**, **18** – ventral and dorsal views of the same specimen showing the migratory cirral anlage in the proter (arrowhead) and the longer dorsal kinety anlagen (double-arrowheads).

with 10 longitudinal dorsal ridges extending over entire length of body, dominant *in vivo* and conspicuous even in stained specimens (Figs 3, 21, arrowheads). Dorsal cilia conspicuous, about 5 μm long; frontoventral cirri strong and about 35–40 μm long. Marginal and caudal cirri relatively fine, with second caudal cirrus longer than the others, and about 40 μm in length (Figs 1, 2, arrows; 23, arrowhead).

Colourless ellipsoidal granules about 2 × 1 μm in size. On an apical view of the dorsal surface, these granules were packed together around the dorsal cilia in a rosette-pattern (Figs 6, 24, arrowheads); on a lateral view of the dorsal surface, the granules protruded out of the cortical surface and were packed like pyramids (Figs 7, 25, arrowheads). On the ventral surface, the granules were packed all around the cirri (Figs 1, 5, arrows). Cytoplasm colourless, transparent in the marginal area but opaque in the central part and packed with many shining globules (ca. 2–3 μm across) and several food vacuoles with possibly flagellates or bacteria. Contractile vacuole not observed. Macronucleus variable in shape: anterior part typically C-shaped, and posterior part curved to distorted (Figs 9–12, 26, arrow). Micronucleus spherical, about 10 μm in diameter, and situated in a depression at the left anterior edge of the macronucleus (Figs 9–12, arrow).

Table 2. Diagnostic traits of *Euplotes dammamensis* n. sp., *E. balteatus* and 18 *Euplotes* species/populations characterized by 10 frontoventral, two left marginal cirri, and several dorsal ridges. Species/population described in the present study are marked in bold.

Species	Body size *in vivo* (μm)	Number of caudal cirri	Number of dorsal kineties	Number of dikineties in mid-dorsal kinety	Feature of dorsal ridges	Number of adoral membranelles	Adoral zone length: body length (%)	Silverline system	Data source
E. dammamensis	**100–170 × 80–120**	**2–3**	**11**	**14–18**	**10, prominent**	**44–51**	**75**	**–**	**Present work**
E. charon	70–100 × 65–90	2–4	9–10	ca. 22	7, conspicucous	51–60	75	Double-eurystomus	Song and Packroff (1997)
E. harpa	150–160	2	13	40–45	10, inconspicuous	65–70	67	Double-eurystomus	Tuffrau (1960)
E. petzi	50–80 × 30–50	2	6	8–10	5, conspicucous	25–33	67	Double-patella	Wilbert and Song (2008)
E. antarcticus	85 × 30	2	8	up to 8	6, clear	ca. 30	67	Double-eurystomus	Fenchel and Lee (1972)
E. euryhalinus	50–62 × 26–38	2–3	10	up to 10	Several, inconspicuous	26–28	67	Double-eurystomus	Valbonesi and Luporini (1990)
E. focardii	38–110 × 30–92	2	10	13–22	2 prominent and 6 inconspicuous	45–65	50–75	Double-eurystomus	Valbonesi and Luporini (1990)
E. balteatus	**70–100 × 50–75**	**2**	**7**	**10–13**	**5, prominent**	**31–39**	**65–75**	**Double-eurystomus**	**Present work**
E. balteatus	60–80	2	–	–	3–5, slight	–	–	–	Kahl (1932)
E. balteatus	30–150	2–3	8	up to 11	–	25–80	67	Double-eurystomus	Tuffrau (1964)
E. balteatus	30–80 × 20–60	2	8	12–16	Ridges inconspicuous	28–43	55–85	Double-eurystomus	Pan *et al*. (2012)
E. wilberti	40–70 × 30–50	2	8–10	9–14	6–7, conspicuous	27–33	67	Double-eurystomus	Song and Wilbert (2002)
E. alatus	75–90	2	–	–	5, conspicuous, the 2nd prominent	–	–	–	Kahl (1932)
E. alatus	40 × 30	2–3	8	10–12	Several, inconspicuous	ca. 26	50	Double-eurystomus	Borror (1968)
E. magnicirratus	51–65 × 36–44	2	8	13–17	Several, distinct	49–52	75	Double-eurystomus	Carter (1972)
E. quinquecarinatus	55 × 40	2	9	13–15	Several, inconspicuous	25–30	50	Double-eurystomus	Borror (1968)
E. plicatum	42–55 × 24–40	2	10	14	7–8, prominent	22–25	67	Double-eurystomus	Valbonesi (1997)
E. trisulcatus	35–50 × 25–40	2	7	7–10	3, prominent	25–36	75	Double-eurystomus	Carter (1972)
E. cristatus	60 × 45	2	8	up to 11	6, prominent	35–47	50–67	Single	Carter (1972)
E. orientalis	35–45 × 20–30	2	6–7	6–8	5–6, conspicuous	18–25	67	Double-patella	Jiang *et al*. (2010)

– Data not available.

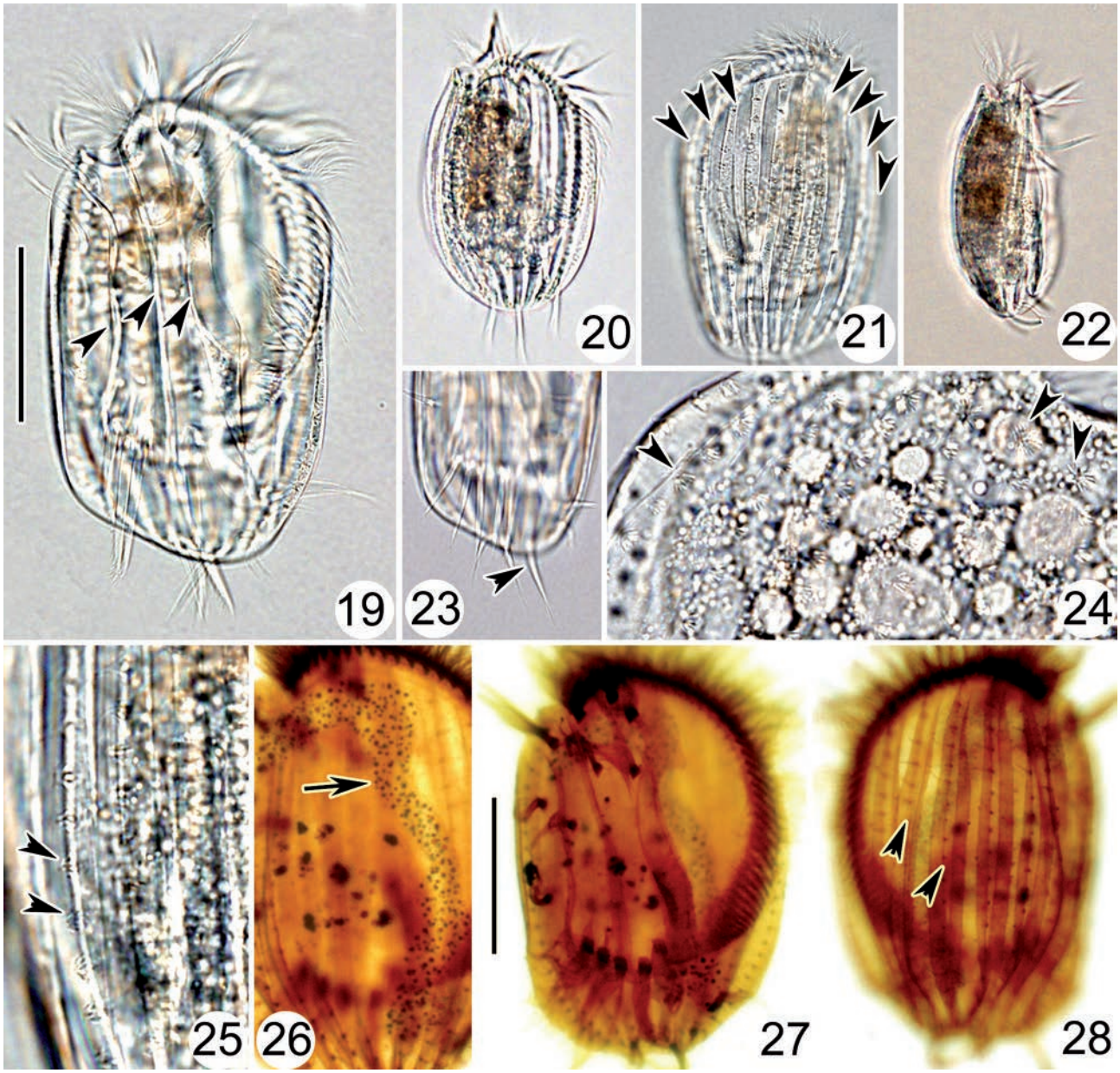

Figs 19–28. Photomicrographs of *Euplotes dammamensis* n. sp. *in vivo* (19–25) and after protargol impregnation (26–28). **19**, **20** – ventral views of different specimens, arrowheads in (19) to show the ventral ridges; **21** – dorsal view, arrowheads point to the dominant dorsal ridges; **22** – lateral view; **23** – ventral view of the posterior end, arrowhead marks the longest caudal cirrus; **24** – detailed dorsal view, arrowheads point to the apical view of the granules around the dorsal brush; **25** – arrowheads to show the lateral view of granules around the dorsal brush; **26** – arrow indicates the curved C-shaped macronucleus; **27**, **28** – infraciliature on the ventral and dorsal sides, arrowheads indicate the dorsal kineties. Scale bars: 50 μm.

Locomotion by crawling slowly on substrate while, occasionally, remaining stationary for rather long periods.

Infraciliature as shown in Figs 8, 9, 26–28. Adoral zone prominent, about three-quarters of total body length and composed of 44–51 membranelles. Paroral membrane about 20 μm in length, typically composed of many irregularly arranged kinetosomes, positioned beneath buccal lip, and generally revealed only by protargol impregnation (Fig. 8). Considering huge body

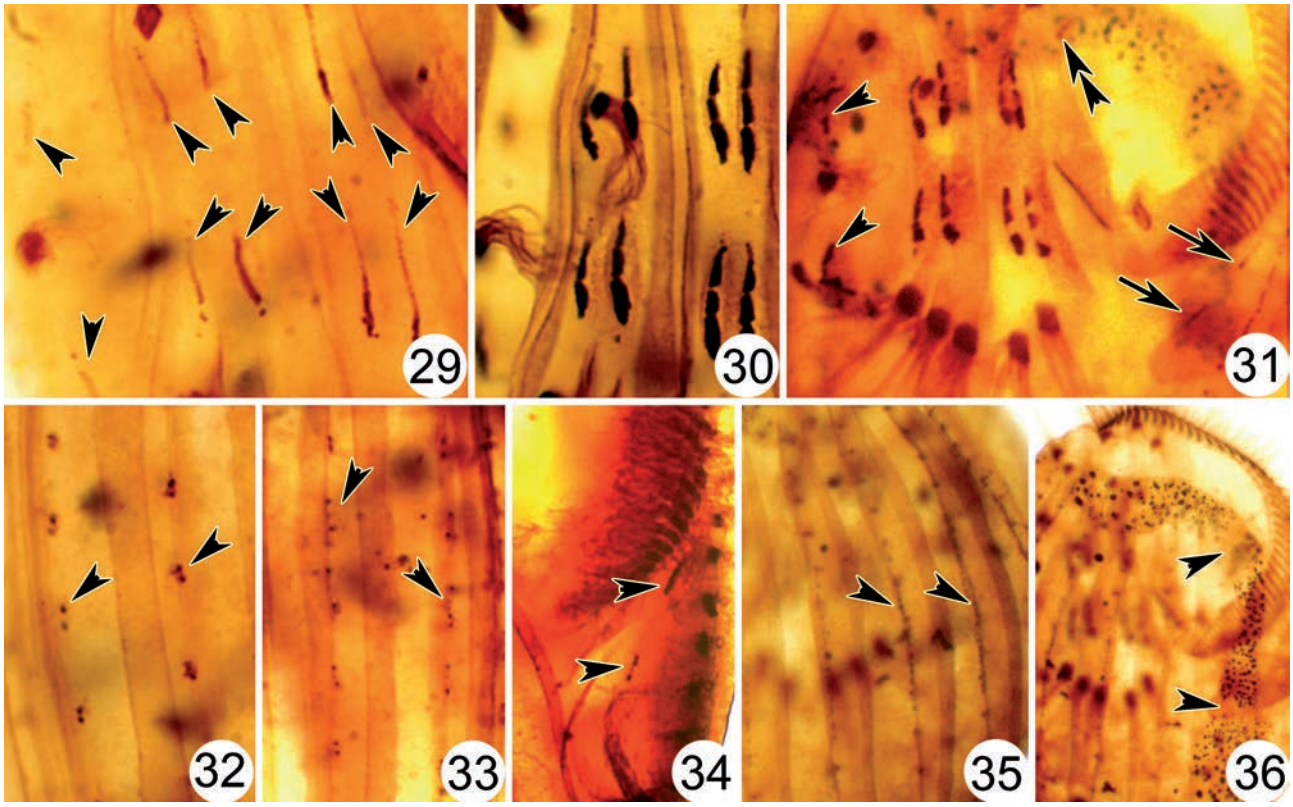

Figs 29–36. Photomicrographs of *Euplotes dammamensis* n. sp. during binary division after protargol impregnation. **29**, **32** – ventral and dorsal views of a specimen at an early stage of morphogenesis to show the frontoventral-transverse cirral anlagen (29, arrowheads) and denote the parental dikinetids (32, arrowheads); **30**, **33**, **34** – ventral and dorsal views of a specimen at a slightly later stage of morphogenesis, to show the frontoventral-transverse cirral anlagen developed and broadened (30), the newly formed dorsal kineties anlagen (33, arrowheads) and the marginal anlagen (34, arrowheads); **31**, **35**, **36** – ventral and dorsal views of a specimen at middle-stage to show the rightmost frontoventral-transverse cirral anlagen (31, arrowheads), the migratory cirral anlage in the proter (31, double-arrowhead), the marginal cirral anlagen (31, arrows), the dorsal kineties anlagen (35, arrowheads) and the replication bands (36, arrowheads).

size, all cirri relatively fine (with their bases usually quite small relative to the ventral surface). Consistently 10 frontoventral cirri arranged in a normal pattern, five strong transverse cirri and two marginal cirri aligned with, usually, two caudal cirri (only five individuals out of 28 observed specimens with three caudal cirri). Always 11 dorsal kineties, extending over the entire length of the cell, except for the leftmost one which started at about the mid-body position and included about 11 dikinetids. Each middle row with about 16 dikinetids, while rightmost and second to rightmost rows with 17–22 and 17–24 dikinetids respectively (Figs 8, 9, 28, arrowheads). The silverline system was unfortunately not able to be obtained.

Morphogenesis. Three specimens were observed in the early and middle stages of morphogenesis and based on this, we can provide some of the morphogenetic features of this new species: 1) the oral primordium in the opisthe developed *de novo* in a subcortical pouch; 2) nine frontoventral and five transverse cirri developed from the five frontoventral transverse anlagen which were formed apokinetally in both daughter cells and then fragmented in a "3:3:3:3:2" pattern; 3) the migratory cirrus in the proter developed *de novo*; 4) the left marginal cirri developed from the marginal anlagen which were formed *de novo*; and 5) the origin of the dorsal kineties anlagen in both daughter cells was in a primary mode, i.e. anlagen for proter and opisthe appeared as one set of densely packed dikinetids (Figs 13–18, 29–36).

Remarks and comparison. This new species can be identified by the characteristics of its cells in both living

and protargol-impregnated specimens although, unfortunately, no silverline system could be revealed. Nonetheless, the species can be unambiguously identified by the combination of the following features: its huge body size, the presence of 10 dominant dorsal ridges, the shape and distribution of the cortical granules, its curved C-shaped macronucleus and, probably, the high salinity of its habitat. It differs from the morphologically closely-related congener, *Euplotes charon* (Müller, 1786) Ehrenberg, 1830, in having a bigger body size (100–170 × 80–120 μm vs. 70–110 × 65–95 μm), more conspicuous dorsal ridges (10 vs. seven) and dorsal kineties (11 vs. 9–10), fewer membranelles (44–51 vs. 51–60) and less dikinetids in the mid-dorsal kinety (ca. 16 vs. ca. 22). It can also be distinguished by the shape of its macronucleus (the anterior part being a typical C-shape but the posterior part being curved to distorted compared to a typical C-shape in *E. charon*), as well as by the shape of its adoral zone, which is even, compared to the proximal portion being conspicuously broad in *E. charon* (Table 2; Song and Packroff 1997). The separation of these two species is also strongly supported by molecular data, since their SSU-rRNA gene sequences differ by 340 nucleotides and exhibit just 80.6% similarity [*E. charon* GenBank accession number: AF492705; submitted by Song (2002)] (Li and Song 2006).

Hitherto, about 16 morphotypes possessing several dorsal ridges, 10 frontoventral, and two left marginal cirri have been reported (Table 2). Besides *Euplotes charon* and *E. dammamensis*, *E. antarcticus* Fenchel and Lee, 1972, *E. petzi* Wilbert and Song, 2008, *E. harpa* Stein, 1859, *E. focardii* Valbonesi and Luporini, 1990 and the Arabian Gulf population of *E. balteatus* also have a big size and a large number of adoral membranelles. We will provide a detailed comparison between *E. dammamensis* and *E. balteatu*s in the following section, here we compare *E. dammamensis* with the other four species listed.

Euplotes antarcticus differs from *E. dammamensis* in its body shape, which is very elongated and almost rectangular in outline except for the pointed posterior region, whereas *E. dammamensis* is approximately rectangular with two rounded ends. *E. antarcticus* also has a smaller body size (85 × 30 μm vs. 100–170 × 100 μm), fewer membranelles (ca. 30 vs. 44–51), fewer dorsal kineties (eight vs. 11) and dorsal ridges (six vs. 10) (Table 2; Fenchel and Lee 1972).

Euplotes petzi has been found, to date, only in the Antarctic area. It differs from *E. dammamensis* in having a smaller body size (50–80 × 30–50 μm vs. 100–170 × 80–120 μm), fewer dorsal kineties (six vs. 11) and dorsal ridges (five vs. 10), and has a sausage shaped or slightly curved macronucleus with closely packed marginal cirri (Table 2; Agatha *et al*. 1993; Petz *et al*. 1995; Wilbert and Song 2008).

Euplotes harpa is also a huge (150–160 μm long) marine *Euplotes* with 10 dominant dorsal ridges. It can be easily distinguished from *E. dammamensis*, however, by the number of its adoral membranelles (65–70 vs. 44–51) and dorsal kineties (13 vs. 11), as well as in having more dikinetids in the mid-dorsal kinety (40–45 vs. ca. 22) (Table 2; Tuffrau 1960). In addition, the SSU-rRNA gene sequences of *E. harpa* and *E. dammamensis* differ in 373 nucleotides and exhibit 78% similarity [*E. harpa* GenBank accession number: AJ305252; submitted by Petroni (2001)] (Petroni *et al*. 2002).

Euplotes focardii was discovered by Valbonesi and Luporini (1990) and is highly variable, both in its size (38–110 × 30–92 μm) and in the number of dikinetids in the mid-dorsal kinety (13–22). It resembles *E. dammamensis* in the number and arrangement of the cirri on the ventral surface and in the ratio of the length of the adoral zone of membranelles to the total body length (50–75% vs. 75%). It also resembles *E. dammamensis* in the number of dorsal kineties (10 vs. 11), dikinetids in the mid-dorsal kinety (13–22 vs. 14–18), and adoral membranelles (45–65 vs. 44–51). *Euplotes focardii* can be distinguished from *E. dammamensis*, however, in the features of its dorsal surface (only the leftmost two ridges are rather pronounced and six other ridges are inconspicuous vs. ten prominent and conspicuous dorsal ridges), the shape of its macronucleus (a typical horseshoe-shaped vs. the anterior part being C-shape but the posterior part being curved to distorted) (Table 2; Valbonesi and Luporini 1990). The divergence of these two forms is supported by SSU-rRNA gene sequence data, as they differ in 351 nucleotides and exhibit 81.3% similarity [*E. focardii* GenBank accession number: EF094960; submitted by Giuseppe and Dini (2006)] (Vallesi *et al.* 2008).

Although *Euplotes neapolitanus* Wichterman, 1964 is also a large marine organism (130 × 70 μm) with 10 frontoventral, two caudal, two left marginal cirri, 11 dorsal kineties, and about 18 dikinetids in the mid-dorsal kinety, it can be easily distinguished from *E. dammamensis* through the absence of dorsal ridges and through the proximal portion of the adoral zone of membranelles being curved at about 90° angle to the right, and being composed of more membranelles (Wichterman 1964).

***Euplotes balteatus* (Dujardin, 1841) Kahl, 1932 (Figs 37–66; Tables 1, 2)**

Some new data, especially in respect to the molecular information, have been obtained from the population studied here and we therefore present an updated description and an improved diagnosis based on present and previous works (Dujardin 1841, Kahl 1932, Tuffrau 1964, Pan *et al*. 2012).

Improved diagnosis. Marine *Euplotes* with 3–5 dorsal ridges, 30–150 × 30–105 μm *in vivo*. Adoral zone about 67–75% of cell length, with 25–80 membranelles. 10 frontoventral, five transverse, 2–3 caudal and two marginal cirri, 7–8 dorsal kineties bearing 10–16 dikinetids in mid-dorsal row. Macronucleus C-shaped or horseshoe-shaped. Micronucleus ellipsoidal, and attached to left arm of macronucleus. Dorsal silverline system in a double-eurystomus pattern.

Voucher slides. Two voucher slides of protargol-stained cells have been deposited in the Laboratory of Protozoology, Ocean University of China, Qingdao (registration number CXR-20111216-21-01, 02).

Morphological description of the Saudi population. Cells *in vivo* usually 70–100 × 50–75 μm in size. Body outline ellipsoidal with anterior and posterior ends slightly narrowed, as shown in Figs 37, 54. Left margin of anterior end truncated in some individuals (Figs 38, 55). Buccal field approximately three-quarters of total cell length. Three conspicuous ridges on ventral side, two right ridges extending posteriorly to transverse cirri, leftmost ridge interrupted by paroral membrane (Figs 37, 38, 55, 57). Five dominant ridges on dorsal side extending over entire cell length (Figs 39, 56, arrowheads).

Cytoplasm colourless, highly transparent at posterior part and oral area, but opaque in central part where it is packed with many different-sized gray granules and a few food vacuoles. Contractile vacuole under the fourth right transverse cirrus (Figs 37, 38, 54, arrow). Macronucleus variable in shape: usually typical horseshoe-shaped (Fig. 44); occasionally, approximately ring-shape, with two ends expanded and almost connected to each other (Fig. 59). Micronucleus spherical, and attached to left arm of macronucleus (Figs 48, 58, arrowhead).

Movement slow, involving crawling on substrate and remaining stationary for long periods.

Cirri and adoral membranelles fine and long. Adoral membranelles, frontoventral, and left marginal cirri approximately 25 μm long, caudal cirri about 20 μm, and transverse cirri 30–35 μm.

Infraciliature as shown in Figs 47, 48, 58–62. Paroral membrane small, typically composed of many irregularly arranged kinetosomes, positioned close to surface of buccal lip and easily revealed *in vivo* (Figs 37, 38, 57, double-arrowheads). Adoral zone of membranelles resembling that of *Euplotes vannus*, proximal portion curved at about 90° angle to right, and composed of 31–39 membranelles. Consistently, 10 frontoventral and five strong transverse cirri forming a normal pattern, two left marginal cirri separated and aligned evenly with two caudal cirri. Seven dorsal kineties extending over almost entire length of cell, with middle row containing 10–13 dikinetids, but leftmost row including only 4–7 dikinetids (Figs 47, 60). Dorsal silverline system in a double-eurystomus pattern (Figs 40, 62).

Morphogenesis. Only one specimen in the middle stage of morphogenesis was obtained. The morphogenesis of this species can be summarized as follows: 1) the oral primordium form in a subcortical pouch; 2) nine frontoventral and five transverse cirri develop from the five frontoventral transverse anlagen which fragment in a "3:3:3:3:2" pattern; 3) the leftmost frontal cirrus develops *de novo* on the cell surface in both dividers; and 4) the left marginal cirri develop from the marginal anlagen which are formed *de novo* (Figs 49, 50, 63–66).

Comparison with different populations. This species was first described by Dujardin (1841) and subsequently redescribed several times (Kahl 1932, Tuffrau 1964, Pan *et al*. 2012). We identify our form by the basic ciliature on the ventral and dorsal surfaces, the marine habitat, the five dorsal ridges, and the double-eurystomus silverline system pattern. Nonetheless, there are some small differences between the Arabian Gulf population and historic populations, such as cell size, the number of dorsal kineties and dikineties in the mid-dorsal kinety, as well as the shape of the macronucleus: for details see Table 2.

The original description was brief and incomplete: oval shaped body with the anterior end slightly narrowed, five inconspicuous dorsal ridges (Dujardin 1841). About a century later, Kahl (1932) gave a good succinct description: cell length about 60–80 μm *in vivo*, dorsoventrally flattened, three to five slight dorsal ridges, ten frontoventral, five transverse, four caudal cirri (Figs 43, 44; Table 2). The morphology of the silverline system and infraciliature were supplied by Tuffrau (1964) (Figs 41, 42, 45; Table 2) and Pan *et al*. (2012) (Figs 46, 51–53; Table 2). In the present Arabian Gulf population, it is noticeable that the five

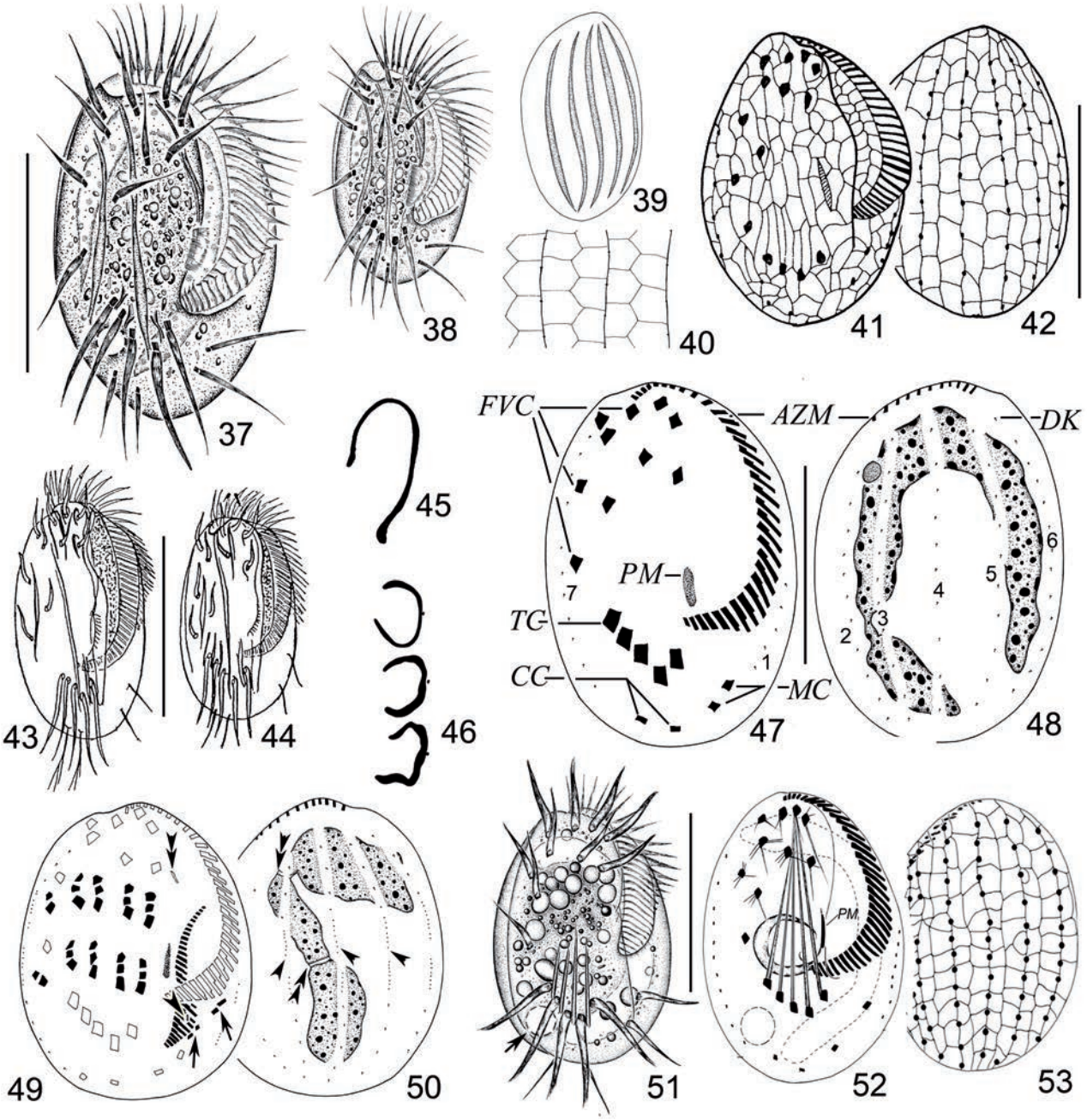

Figs 37–53. *Euplotes balteatus in vivo* (37–39, 43, 44, 51), after silver nitrate (41, 42, 45, 52, 53) and protargol (40, 46, 47–50) impregnation. **37**, **38**, **43**, **44**, **51** – ventral views of different individuals (43, 44 from Kahl 1932; 51 from Pan *et al*. 2012); **39** – dorsal view, showing the five conspicuous ridges; **40** – double-eurystomus type of silverline system on the dorsal side; **41**, **42**, **52**, **53** – silverline system on the ventral and dorsal sides (41, 42 after Tuffrau 1964; 52, 53 from Pan *et al*. 2012); **45** – macronucleus hook-shaped (from Tuffrau 1964); **46** – macronucleus horseshoe-shaped (from Pan *et al*. 2012); **47**, **48** – ventral and dorsal views of the infraciliature; **49**, **50** – ventral and dorsal views of an middle divider, showing the frontoventral-transverse cirral anlagen, the migratory cirri anlagen in the proter (49, double-arrowhead) and opisthe (49, arrowhead), the marginal cirral anlagen (49, arrows), the dorsal kineties anlagen (50, arrowheads) and the replication bands (50, double-arrowheads). AZM – adoral zone of membranelle, CC – caudal cirri, DK – dorsal kineties, FVC – frontoventral cirri, MC – marginal cirri, PM – paroral membrane, TC – transverse cirri, 1–7 – dorsal kineties. Scale bars: 50 μm.

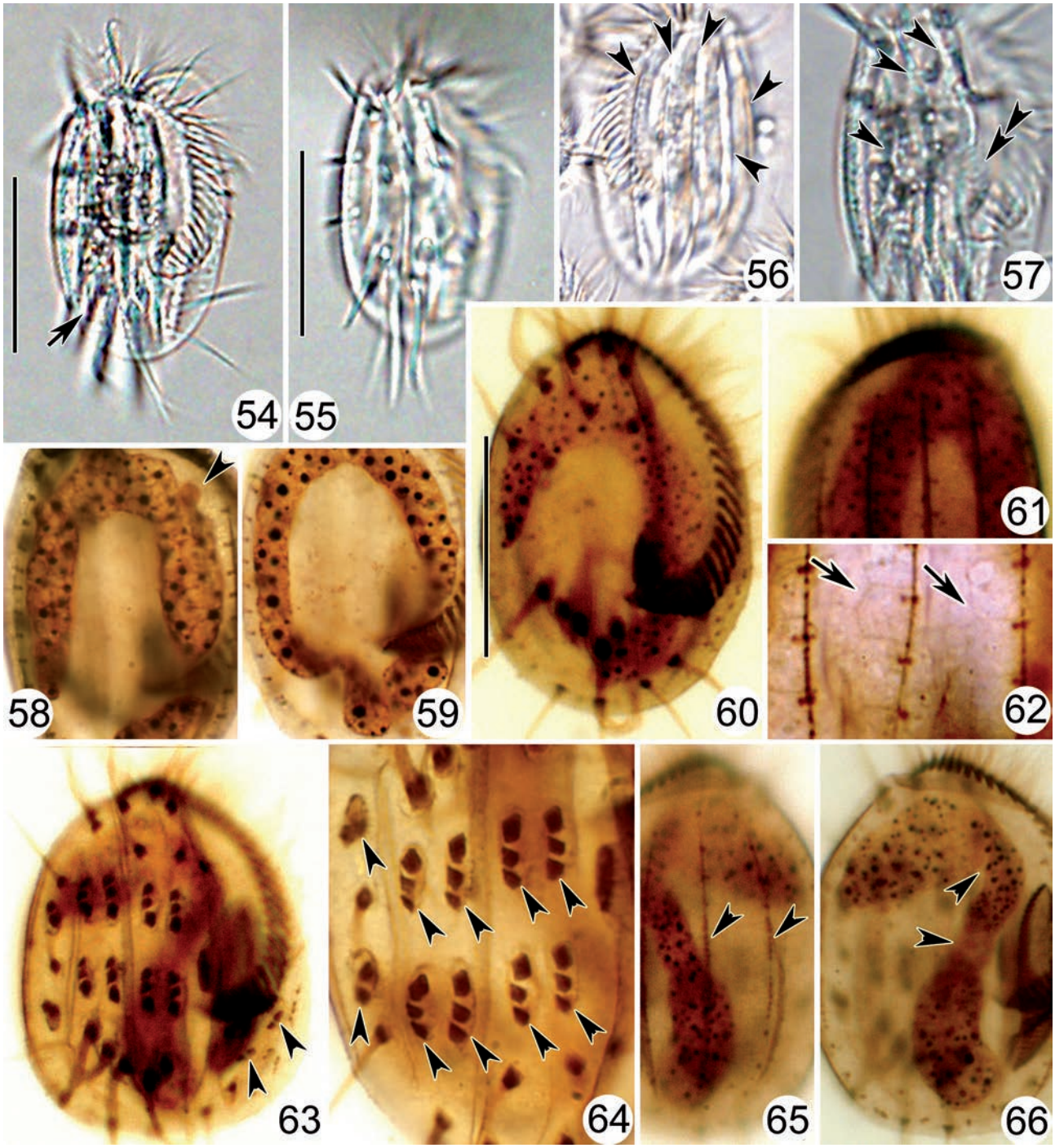

Figs 54–66. Photomicrographs of *Euplotes balteatus in vivo* (54–57) and after protargol-impregnation (58–66). **54**, **55** – ventral views of different individuals, arrow (54) denotes the contractile vacuole; **56** – dorsal view, arrowheads mark dominant ridges; **57** – ventral view, arrowheads mark ventral ridges, double-arrowhead denote paroral membrane; **58**, **59** – different shapes of macronucleus, arrowhead (58) marks the micronucleus; **60**, **61** – infraciliature on the ventral and dorsal sides; **62** – double-eurystomus type of silverline system on the ventral side; **63–66** – ventral and dorsal views of an early divider, showing the marginal cirral anlagen (63, arrowheads), frontoventral-transverse cirral anlagen (64, arrowheads), the dorsal kineties anlagen (65, arrowheads), and replication bands (66, arrowheads). Scale bars: 50 μm.

dorsal ridges are dominant. Because this diagnostic trait usually varies in relation with the cell's nutritive conditions, it is regarded as a population-level difference.

Supposed synonym. In the original description (Kahl 1932), *Euplotes alatus* is a medium marine species (75–90 μm long) with 10 frontoventral, two caudal, and two marginal cirri, and five conspicuous dorsal ridges (the leftmost 2nd ridge being huge and prominent). In Borror's redescription, it has eight dorsal kineties, 10–12 dikinetids in the mid-dorsal kinety, about 26 adoral membranelles, and the double-eurystomus silverline system pattern (Table 2; Figs 67–72; Borror 1968). We incline to consider these characters as interspecific differences and agree with Song and Wilbert (2002) that *E. alatus* is possibly a junior synonym of *E. balteatus*. For the same reason, *E. quinquecarinatus* Borror, 1968 may also be a junior synonym of *E. balteatus* (Table 2; Figs 80–83; Borror 1968, Song and Wilbert 2002).

Comparison with related congeners. In terms of the 10 frontoventral, two caudal, two marginal cirri, and several dorsal ridges, there are ten potentially related species

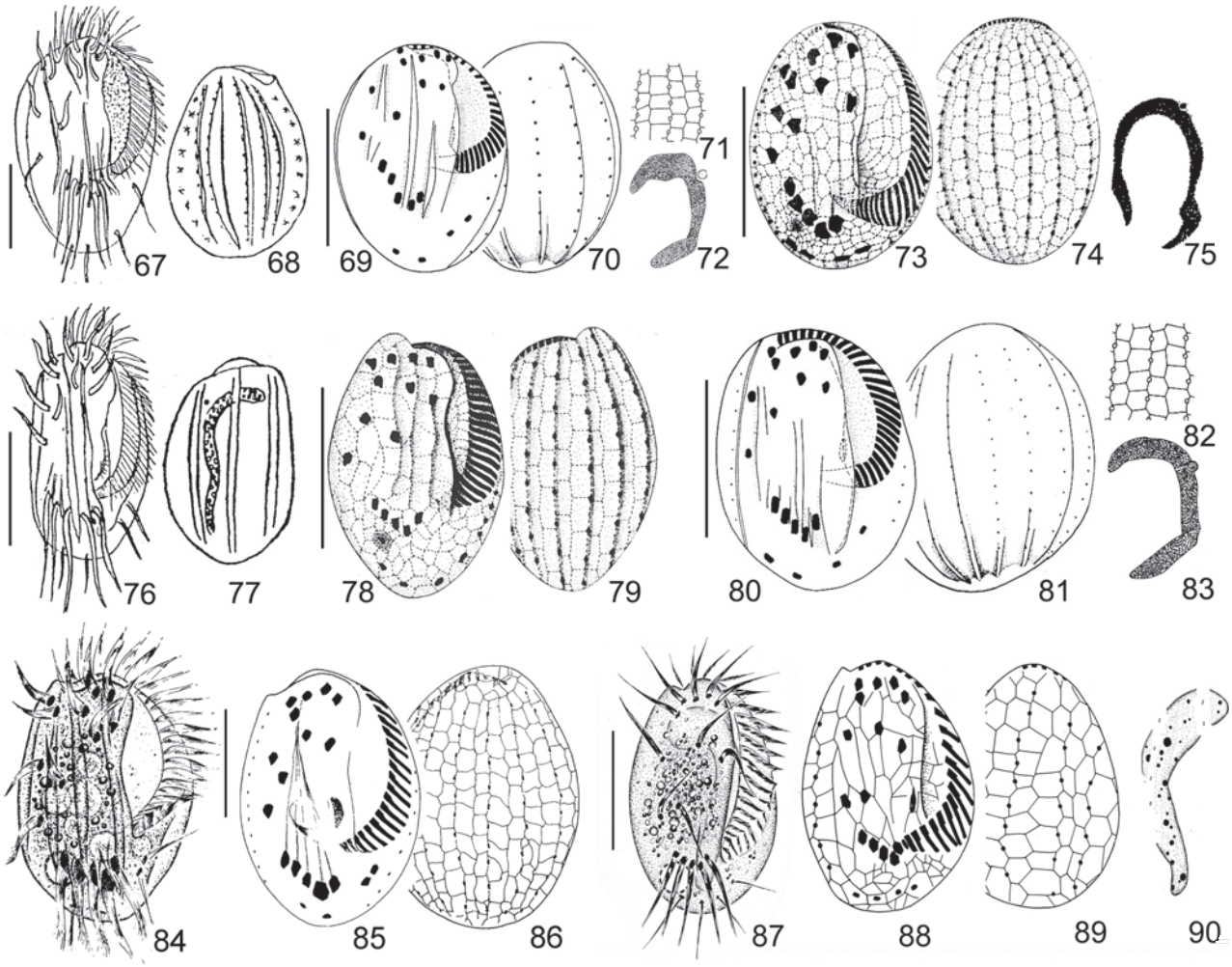

Figs 67–90. Morphologically similar marine *Euplotes* species with double-eurystomus silverline system pattern, and 10 frontoventral, two caudal, two marginal cirri. **67–72** – *E. alatus* Kahl, 1932 (67, 68 from Kahl 1932; 69–72 from Borror 1968); **73–75** – *E. magnicirratus* Carter, 1972 (from Carter 1972); **76–79** – *E. trisulcatus* Kahl, 1932 (76, 77 from Kahl 1932; 78, 79 from Carter 1972); **80–83** – *E. quinquecarinatus* Gelei, 1950 sensu Borror (1968) (from Borror 1968); **84–86** – *E. wilberti* Pan *et al*., 2012 (from Song and Wilbert 2002); **87–90** – *E. parabalteauts* Jiang *et al*., 2010 (from Jiang *et al*. 2010a). Scale bars: 25 μm.

Table 3. The alignment results of SSU-rRNA gene sequence of 11 *Euplotes* species. Numbers in the lower diagonal are similarities between the two species (%), while those in the upper diagonal are the numbers of the different nucleotides between the two species.

Species name	*E. par*	***E. dam***	*E. har*	*E. eur*	***E. bal***	*E. ori*	*E. pli*	*E. tri*	*E. foc*	*E. cha*	*E. mag*
E. par	–	176	358	358	317	314	313	342	311	299	295
E. dam	89.7	–	411	412	368	367	367	388	351	356	352
E. har	80.7	78.5	–	162	204	199	200	197	175	183	179
E. eur	80.4	78.2	91.5	–	228	221	222	212	205	203	199
E. bal	82.3	80.2	89.2	87.8	–	18	14	196	167	169	165
E. ori	82.5	80.2	89.5	88.2	99.0	–	6	188	163	167	163
E. pli	82.5	80.2	89.4	88.1	99.2	99.7	–	188	163	165	161
E. tri	81.2	79.4	89.7	88.7	89.5	90.0	90.0	–	140	125	121
E. foc	82.8	81.3	90.8	89.1	91.0	91.2	91.2	92.5	–	128	124
E. cha	83.4	80.9	90.4	89.2	90.9	91.0	91.1	93.3	93.1	–	4
E. mag	83.6	81.1	90.5	89.3	91.1	91.2	91.3	93.5	93.3	99.8	–

E. par – *E. parabalteatus*, *E. dam* – *E. damammensis* n. sp, *E. har* – *E. harpa*, *E. eur* – *E. eurystomus*, *E. bal* – *E. balteatus*, *E. ori* – *E. orientalis*, *E. pli* – *E. plicatum*, *E. tri* – *E. trisulcatus*, *E. foc* – *E. focardii*, *E. cha* – *E. charon*, *E. mag* – *E. magnicirratus*. Species described in the present study are marked in bold.

that should be compared with *E. balteatus*: *E. trisulcatus* Kahl, 1932; *E. cristatus* Kahl, 1932, sensu Tuffrau (1960), *E. magnicirratus* Carter, 1972, *E. euryhalinus* Valbonesi and Luporini, 1990, *E. plicatum* Valbonesi *et al*., 1997, *E. petzi* Wilbert and Song, 2008, *E. orientalis* Jiang *et al*., 2010, *E. wilberti* Pan *et al*., 2012, *E. parabalteatus* Jiang *et al*., 2010, *E. dammamensis* n. sp. (Table 2). Of these, *E. cristatus* differs from *E. balteatus* in its single-vannus silverline system pattern (Tuffrau 1960). For the same reason, *E. orientalis* and *E. petzi* can be easily distinguished from *E. balteatus* through their double-patella silverline system pattern (Petz *et al*. 1995, Wilbert and Song 2008, Jiang *et al*. 2010b).

Euplotes magnicirratus is similar to *E. balteatus* in its cell size, the basic ciliature on both ventral and dorsal sides, the marine habitat, and the features of its dorsal ridges. The former differs from the latter, however, in having more adoral membranelles (49–52 vs. generally 25–39) and, particularly, stronger cirri on the ventral side (Table 2; Figs 73–75; Carter 1972). In addition, the SSU-rRNA gene sequences of *E. magnicirratus* and *E. balteatus* differ in 165 nucleotides and exhibit 91.1% similarity [*E. magnicirratus* GenBank accession number: AJ549210; submitted by Petroni (2003)] (Table 3; Petroni *et al*. 2002).

Euplotes plicatum is a small (42–55 × 24–40 μm) organism collected from the harbour of Lyttelton (Christchurch, New Zealand) whose diagnosis closely resembles that of *E. balteatus*: marine habitat, 10 frontoventral, five transverse, two caudal, and two marginal cirri, 22–25 adoral membranelles, double-eurystomus silverline system pattern (Table 2; Valbonesi *et al*. 1997). It can be distinguished from *E. balteatus*, however, through several morphological differences, i.e. the number of dorsal ridges (7–8 vs. 3–5) and dorsal kineties (10 vs. 7–8). Also, the SSU-rRNA gene sequences of the two species differ in 14 nucleotides and exhibit 99.2% similarity [*E. plicatum* GenBank accession number: EF094966; submitted by Giuseppen and Dini (2006)] (Table 3; Vallesi *et al*. 2008).

Euplotes euryhalinus differs from *E. balteatus* in having more dorsal kineties (11 vs. generally 7–8), and more dikinetids in the mid-dorsal kinety (18 vs. 10–16) (Table 2; Valbonesi and Luporini 1990). The two species can also be easily distinguished by their molecular information, with 228 different nucleotides between their SSU-rRNA gene sequences and a similarity of 87.8% [*E. euryhalinus* GenBank accession number: EF094968; submitted by Giuseppen and Dini (2006)] (Table 3; Vallesi *et al*. 2008).

Euplotes parabalteatus is similar to *E. balteatus* in cell shape and size, cirral pattern and silverline system. The former, however, can be separated from the latter by the feature of dorsal ridges (absent vs. 3–5 conspicuous), having fewer adoral membranelles (19–23 vs. 25–80) and dorsal kineties (6–7 vs. 7–8), the shape of

macronucleus (slightly curved-bar-shaped vs. inverted C-shaped) (Figs 87–90; Jiang *et al*. 2010a). The divergence of these two forms is supported by SSU-rRNA gene sequence data, as they differ in 317 nucleotides and exhibit 82.3% similarity [*E. parabalteatus* GenBank accession number: FJ346568; submitted by Li and Song (2008)] (Table 3; Jiang *et al.* 2010a).

Euplotes wilberti was collected from King George Island, Antarctica and originally reported by Song and Wilbert (2002) as another population of *E. balteatus*. The Antarctica population differs from *E. balteatus* in several respects, however, including: the number of dorsal ridges (6–7 vs. 3–5) and dorsal kineties (8–10 vs. 7–8) and the character of the marginal cirri (densely ranged vs. widely separated). Based on these differences, Pan *et al*. (2012) identified it as a new species, *E. wilberti* (Figs 84–86; Table 2; Song and Wilbert 2002, Pan *et al*. 2012).

Euplotes trisulcatus is a "slim" organism, with a ratio of body length to width of about 2:1. It differs from *E. balteatus* in two respects: the number of dorsal ridges (stable three vs. 3–5) and the shape of the macronucleus (slightly curved vs. inverted C-shaped) (Figs 76–79; Table 2; Kahl 1932, Tuffrau 1960). Based on these morphological features alone it should be synonymised with *E. balteatus*. The SSU-rRNA gene sequences of the two species, however, differ in 196 nucleotides and exhibit 89.5% similarity [*E. trisulcatus* GenBank accession number: EF690810; submitted by Schwarz and Stoeck (2007); unpublished] (Table 3). In view of this, detailed redescription of *E. trisulcatus* is necessary, especially to ensure that the morphometric and molecular data are based on the same population.

Euplotes dammamensis, meanwhile, the new species described in this work, can be clearly distinguished from the present population of *E. balteatus* by its body size (100–170 μm vs. 60–100 μm), the number of dorsal ridges (10 vs. 3–5), and dorsal kineties (11 vs. 7–8) (Table 2). The dissimilarity between them is also supported by the molecular data, since their SSU-rRNA gene sequences differ by 337 nucleotides and exhibit 80.3% similarity (Table 3).

Phylogenetic analyses of two *Euplotes* species based on SSU-rRNA gene sequences

The ML and BI trees showed an identical topological structure (Fig. 91). *Euplotes* spp. formed a well-supported clade (ML 100%, BI 1.00). As shown in Fig. 91, this group includes six well-supported clades and several species for which relationships remain unresolved. This is consistent with results presented in previous SSU-rRNA trees (Yi *et al*. 2009; Jiang *et al*. 2010a, b). The new species, *E. dammamensis* n. sp., did not cluster with the morphologically similar species *E. charon*. In fact, it clustered with a small-sized *E. parabalteatus* without any dorsal ridges, together with *E. sinicus* branching independently at the basal position for all other *Euplotes* species. The phylogenetic analyses presented here, along with the comparisons of the nucleotide sequences of the SSU-rRNA gene regions, support the validity of *E. dammamensis*, *E. charon*, *E. harpa*, and *E. focardii* as distinct species. The newly sequenced *Euplotes balteatus* clusters with *E. plicatum* and *E. orientalis* with high support value (ML 100%, BI 1.00) and, together with *E. bisulcatus*, form one of the major clade with full support (ML 100%, BI 1.00). Although these four species grouped together, *E. bisulcatus* has a different cirral pattern (nine frontoventral cirri and single marginal cirrus), and *E. orientalis* has a different dorsal silverline system type (double-patella), as mentioned above. It is noteworthy that five morphologically similar species, *E. balteatus*, *E. plicatum*, *E. magnicirratus, E. euryhalinus*, and *E. parabalteatus* did not cluster in a group, which tends to support the opinion of Petroni *et al*. (2002), Schwarz *et al*. (2007), and Yi *et al*. (2009) that phylogenetic reconstructions of the *Euplotes* species based on molecular evidence in some cases disagree with taxonomic classifications and phylogenetic reconstructions based on morphological characters (e.g. dorsal argyrome pattern).

Acknowledgements. Our deep thanks are expressed to the anonymous reviewers and editors for their helpful criticisms and comments on the first version of this manuscript. The research was sponsored by the Natural Science Foundation of China (project Nos. 41006086 to Chen; 31172041 to Shao), King Saud University, Deanship of Scientific Research, Research Group Project (No. RGP-VPP-083), the Discipline Project of Ningbo University (Nos. xkc11006; xkl11102) and K. C. Wong Magna Fund in Ningbo University. We also thank Prof. Weibo Song (Ocean University of China) and Dr. Zhenzhen Yi (South China Normal University) for their constructive suggestions and modifications to the manuscript.

REFERENCES

Agatha S., Spindler M., Wilbert N. (1993) Ciliated protozoa (Ciliophora) from Arctic sea ice. *Acta Protozool*. **32:** 261–278

Agatha S., Wilbert N., Spindler M., Elbrächter M. (1990) Euplotide ciliates in sea ice of the Weddell Sea (Antarctica). *Acta Protozool.* **29:** 221–228

Berger H., Foissner W. (1989) Morphology and biometry of some soil hypotrichs (Protozoa, Ciliophora) from Europe and Japan. *Bull. Br. Mus. Nat. Hist. (Zool.)* **55:** 19–46

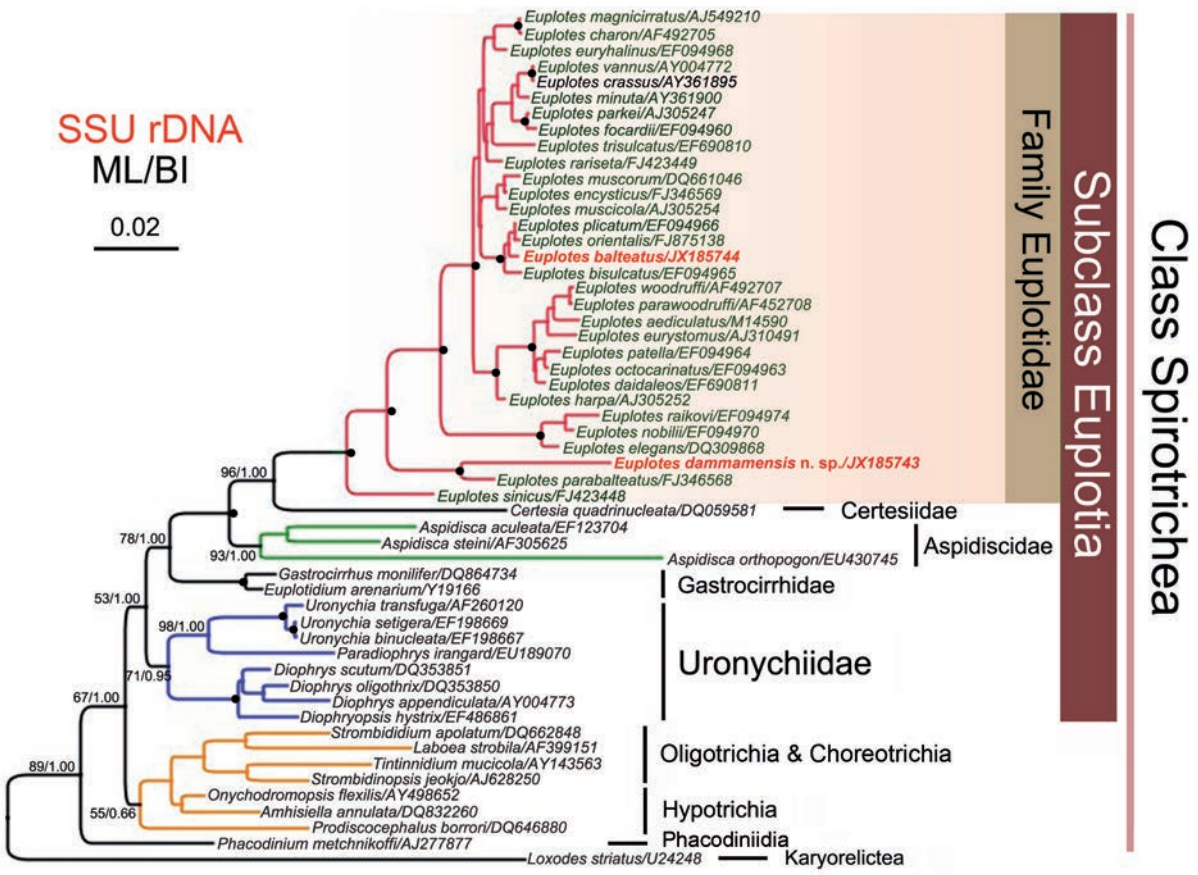

Fig. 91. Phylogenetic tree inferred by Maximum Likelihood (ML) based on SSU-rRNA gene sequences, showing the positions of *Euplotes dammamensis* n. sp. and *Euplotes balteatus* (red highlighted). The topology of the tree constructed with Bayesian analysis (BI) was essentially identical. Fully supported (100%/1.00) branches are marked with solid circles. The scale bar corresponds to 2 substitutions per 100 nucleotide positions. Systematic classification follows Lynn (2008).

Borror A. C. (1968) Systematics of *Euplotes* (Ciliophora, Hypotrichia); toward union of the old and the new. *J. Protozool.* **15:** 802–808

Borror A. C. (1972) Revision of the order Hypotrichida (Ciliophora, Protozoa). *J. Protozool.* **19:** 1–23

Carter H. P. (1972) Infraciliature of eleven species of the genus *Euplotes*. *Trans. Am. Microsc. Soc.* **91:** 466–492

Chen X., Gao S., Liu W., Song W., Al-Rasheid K., Warren A. (2012) Taxonomic descriptions of three marine colepid ciliates, *Nolandia sinica* spec. nov., *Apocoleps caoi* spec. nov. and *Tiarina fusa* (Claparède & Lachmann, 1858) Bergh, 1881 (Ciliophora, Prorodontida). *Int. J. Syst. Evol. Microbiol.* **62:** 735–744

Coppellotti O., Cisotto P. (1996) Description of *Euplotes margherensis* nov. spec. (Ciliophora, Hypotrichida) from the Lagoon of Venice. *Ital. J. Zool.* **63:** 163–167

Curds C. R. (1975) A guide to the species of the genus *Euplotes* (Hypotrichida, Ciliatea). *Bull. Br. Mus. Nat. Hist. (Zool.)* **28:** 3–61

Drummond A., Ashton B., Buxton S., Cheung M., Cooper A., Heled J. *et al*. (2010) Geneious v5. 1. In: Biomatters. Ltd. Auckland, New Zealand

Dujardin F. (1841) Histoire Naturelle des Zoophytes. In: Infusoires. Paris

Fenchel T., Lee C. C. (1972) Studies on ciliates associated with the sea ice from Antarctica. I. The nature of the fauna. *Arch. Protistenk.* **114:** 231–236

Guindon S., Gascuel O. (2003) A simple, fast and accurate algorithm to estimate large phylogenies by maximum likelihood. *Sys. Biol.* **52:** 696–704

Huang J., Dunthorn M., Song W. (2012) Expanding character sampling for the molecular phylogeny of euplotid ciliates (Protozoa, Ciliophora) using three markers, with a focus on the family Uronychiidae. *Mol. Phylogent. Evol.* **63:** 598–605

Jiang J., Zhang Q., Hu X., Shao C., Al-Rasheid K., Song W. (2010a) Two new marine ciliates, *Euplotes sinicus* sp. nov. and *Euplotes parabalteatus* sp. nov., and a new small subunit rRNA gene sequence of *Euplotes rariseta* (Ciliophora, Spirotrichea, Euplotida). *Int. J. Syst. Evol. Microbiol.* **60:** 1241–1251

Jiang J., Zhang Q., Warren A., Al-Rasheid K., Song W. (2010b) Morphology and SSU rRNA gene-based phylogeny of two marine *Euplotes* species, *E. orientalis* spec. nov. and *E. raikovi*

Agamaliev, 1966 (Ciliophora, Euplotida). *Eur. J. Protistol.* **46:** 121–132

Kahl A. (1932) Urtiere oder Protozoa. I: Wimpertiere oder Ciliata (Infusoria) 3. Spirotricha. *Tierwelt Dtl.* **25:** 399–650

Li L., Song W. (2006) Phylogenetic position of the marine ciliate, *Certesia quadrinucleata* (Ciliophora; Hypotrichia; Hypotrichida) inferred from the complete small subunit ribosomal RNA gene sequence. *Eur. J. Protistol*. **42:** 55–61

Lobban C. S., Modeo L., Verni F., Rosati G. (2005) *Euplotes uncinatus* (Ciliophora, Hypotrichia), a new species with zooxanthelae. *Mar. Biol.* **147:** 1055–1061

Lynn D. H. (2008) The Ciliated Protozoa: Characterization, Classification, and Guide to the Literature, 3rd ed. Springer, Dordrecht

Medlin L., Elwood H. J., Stickel S., Sogin M. L. (1988) The characterization of enzymatically amplified eukaryotic 16S-like rRNA-coding regions. *Gene* **71:** 491–499

Nylander J. (2004) MrModeltest v2. Program distributed by the author. In: Evolutionary Biology Centre, Uppsala University

Pan Y., Li L., Shao C., Hu X., Ma H., Al-Rasheid K., Warren A. (2012) Morphology and ontogenesis of a marine ciliate, *Euplotes balteatus* (Dujardin, 1841) Kahl, 1932 (Ciliophora, Euplotida) and definition of *Euplotes wilberti* nov. spec. *Acta Protozool*. **51:** 29–38

Petroni G., Dini F., Verni F., Rosati G. (2002) A molecular approach to the tangled intrageneric relationships underlying phylogeny in *Euplotes* (Ciliophora, Spirotrichea). *Mol. Phylogenet. Evol.* **22:** 118–130

Petz W., Song W., Wilbert N. (1995) Taxonomy and ecology of the ciliate fauna (Protozoa, Ciliophora) in the endopagial and pelagial of the Weddel Sea, Antarctica. *Stapfia* **40:** 1–223

Posada D., Crandal K. A. (1998) Modeltest: testing the model of DNA substitution. *Bioinformatics* **14:** 817–818

Ronquist F., Huelsenbeck J. P. (2003) MRBAYES 3: Bayesian phylogenetic inference under mixed models. *Bioinformatics* **19:** 1572–1574

Schwarz M. V. J., Stoeck T. (2007) *Euplotes pseudoelegans* n. sp. (Hypotrichida; Euplotidae): description of a new species previously misidentified as *Eplotes elegans* Kahl, 1932. *Acta Protozool.* **46:** 193–200

Schwarz M. V. J., Zuendorf A., Stoeck T. (2007) Morphology, ultrastructure, molecular phylogeny, and autecology of *Euplotes elegans* Kahl, 1932 (Hypotrichida; Euplotidae) isolated from the anoxic Mariage Fjord, Denmark. *J. Eukaryot. Microbiol.* **54:** 125–136

Shao C., Ma H., Gao S., Al-Rasheid K., Song W. (2010) Reevaluation of cortical developmental patterns in *Euplotes* (s.l.), including a morphogenetic redescription of *E. charon* (Protozoa, Ciliophora, Euplotida). *Chin. J. Oceanol. Limnol.* **28:** 593–602

Song W., Bradbury P. (1997) Comparative studies on a new brackish water *Euplotes*, *E. parawoodruffi* n. sp., and a redescription of *Euplotes woodruffi* GAW, 1939 (Ciliophora; Hypotrichida). *Arch. Protistenkd.* **148:** 399–412

Song W., Packroff G. (1997) Taxonomische Untersuchungen an marinen Ciliaten aus China mit Beschreibungen von zwei neuen Arten, *Strombidium globosaneum* nov. spec. und *S. platum* nov. spec. (Protozoa, Ciliophora). *Arch. Protistenkd.* **147:** 331–360

Song W., Wilbert N. (1997) Morphological investigations on some free living ciliates (Protozoa, Ciliophora) from China Sea with description of a new hypotrichous genus, *Hemigastrostyla* nov. gen. *Arch. Protistenkd*. **148:** 413–444

Song W., Wilbert N. (2002) Faunistic studies on marine ciliates from the Antarctic benthic area, including descriptions of one epizoic form, 6 new species and 2 new genera (Protoza; Ciliophora). *Acta Protozool.* **41:** 23–61

Tamura K., Peterson D., Peterson N., Stecher G., Nei M., Kumar S. (2011) MEGA5: molecular evolutionary genetics analysis using maximum likelihood, evolutionary distance, and maximum parsimony methods. *Mol. Biol. Evol.* **28:** 2731–2739

Tuffrau M. (1960) Révision du genre *Euplotes*, fondée sur la comparaison des structures superficielles. *Hydrobiologia* **15:** 1–77

Tuffrau M. (1964) Le maintien des caractères spécifiques à travers le polymorphisme d'*Euplotes balteatus* Dujardin, 1841. *Arch. Zool. Exp. Gén.* **104:** 143–151

Valbonesi A., Apone F., Luporini P. (1997) Morphology and biology of a new species of *Euplotes*, *Euplotes plicatum* sp. n. (Ciliophora: Euplotidae). *Acta Protozool.* **36:** 287–294

Valbonesi A., Luporini P. (1990) Description of two new species of *Euplotes* and *Euplotes rariseta* from Antarctica. *Polar Biol.* **11:** 47–53

Valbonesi A., Luporini P. (1995) *Euplotes bisulcatus*, a key species for a better understanding of the organization and evolution of *Euplotes argyrome* patterns. *Eur. J. Protistol.* **31:** 32–37

Valbonesi A., Ortenzi C., Luporini P. (1987) Observations on the biology of *Euplotes charon* (Hypotrichda, Ciliophora). *Bull. Zool*. **54:** 111–118

Vallesi A., Giuseppe G. D., Dini F., Luporini P. (2008) Pheromone evolution in the protozoan ciliate, *Euplotes*: the ability to synthesize diffusible forms is ancestral and secondarily lost. *Mol. Phylogenet. Evol.* **47:** 439–442

Wichterman E. (1964) Descriptions and life cycle of *Euplotes neapolitanus* sp. nov. (Protozoa, Ciliophora, Hypotrichida) from the Gulf of Naples. *Trans. Am. Microsc. Soc.* **83:** 362–370

Wilbert N. (1975) Eine verbesserte Technik der Protargolimprägnation für Ciliaten. *Mikrokosmos* **64:** 171–179

Wilbert N., Song W. (2008) A further study on littoral ciliates (Protozoa, Ciliophora) near King George Island, Antarctica, with description of a new genus and seven new species. *J. Nat. Hist.* **42:** 979–1012

Yi Z., Song W., Clamp J., Chen Z., Gao S., Zhang Q. (2009) Reconsideration of systematic relationships within the order Euplotida (Protista, Ciliophora) using new sequences of the gene coding for small-subunit rRNA and testing the use of combined data sets to construct phylogenies of the *Diophrys*-like species. *Mol. Phylogen. Evol.* **50:** 599–607

Submitted on 1st November, 2012; revised on 28th January, 2012; accepted on 11th March, 2013